Effect of Radiation Power Loss due to Impurity Gas Puff on Divertor Plasma*)

Izumi MURAKAMI, Daiji KATO, Hiroyuki A. SAKAUE and Suguru MASUZAKI

National Institute for Fusion Science, 322-6 Oroshi-cho, Toki 509-5292, Japan

(Received 27 December 2010 / Accepted 28 February 2011)

In order to examine the effect of radiation power loss due to impurity gas puff in divertor plasma, we calculated time evolution of impurity ion densities and electron temperature for several cases with Ne gas puff rates 10^{12} and 10^{13} cm^{-3}s^{-1} during 0.01 s and initial electron temperature 10-300 eV for a plasma with electron density 10^{13} cm^{-3} with a one zone model. We found that the electron temperature decreases less than 1 eV for the cases with gas puff rate 10^{13} cm^{-3}s^{-1}, independent of initial electron temperature and in this case we expect plasma detachment. Detailed conditions for plasma detachment should also depend on time history of radiation power.

Keywords: gas divertor, radiation power loss, Ne, atomic process

DOI: 10.1585/pfr.6.2403029

1. Inroduction

Reducing high heat load on a divertor plate is an issue to prevent serious damage to divertor plates in future fusion devices such as the ITER, a DEMO and a LHD-type reactor (FFHR) [1]. Gas injection (puffing) into a divertor plasma is one possible idea to reduce the heat load on divertor plates, since impurity gas causes radiative power loss and decreases electron temperature, expected to result in plasma detachment. The effect of impurity radiation loss was examined analytically for the ITER divertor [2–4] and neon was found to be the optimum candidate. There are several studies of the effect of gas injection (puffing) for the scrape-off layer and divertor region for ITER [5,6] and JT-60SA [7] using transport codes. In Ref. [6] a time dependent feature was predicted for large impurity fractions, and the oscillatory behavior was attributed to a cyclic conversion of neutrals into ions and then back to neutrals near the divertor plate.

In this work we examine the effect of radiation power loss produced by impurity gas puffs in a divertor plasma. We perform time-dependent calculations of impurity ion densities and electron temperature and examine whether plasma detachment will be likely or not. We mainly investigate neon gas puff cases, and also perform a preliminary calculation for a nitrogen gas puff and discuss the results.

2. Model

Here we consider a one zone model and ignore spatial distribution of electron temperature and density, hydrogen density and impurity density to examine simply the effect of radiation power loss to a plasma. We calculate time dependent ion and atom densities of the injected impurity gas and bulk hydrogen. The ion and atom densities are changed by electron-impact ionization and recombination processes. The ion number density of i-th charged state $n(i)$ is obtained as

$$\frac{\mathrm{d}n(i)}{\mathrm{d}t} = S(i-1)n(i-1)n_\mathrm{e} - S(i)n(i)n_\mathrm{e} - \alpha(i)n(i)n_\mathrm{e} + \alpha(i+1)n(i+1)n_\mathrm{e}, \quad (1)$$

where $S(i)$ is ionization rate of i-th ion to be (i+1)-th ion, $\alpha(i)$ is recombination rate from i-th ion to (i-1)-th ion, and n_e is electron density. Both radiative and dielectronic recombination processes are considered. Three-body recombination is ignored in this work, since this process is not effective for electron temperatures larger than 1 eV. Electron-impact ionization and dielectronic recombination rate coefficients are taken from Refs. [8] and [9], respectively. Radiative recombination rate coefficients are calculated with a Fortran subroutine written by D. Verner [10].

The electron temperature T_e is calculated with the energy conservation equation approximated as

$$\frac{3}{2}n_\mathrm{e}k\frac{\mathrm{d}T_\mathrm{e}}{\mathrm{d}t} \approx -\sum_i L_\mathrm{tot}(i)n(i)n_\mathrm{e}, \quad (2)$$

$$L_\mathrm{tot}(i) = L_{LT}(i) + L_{RB}(i), \quad (3)$$

where$L_{LT}(i)$ and $L_{RB}(i)$ are radiation power coefficients due to line transitions, and radiative recombination and Bremsstrahlung, respectively. Atomic data of the radiation power coefficients are taken from ADAS [11] and the density effect is included in the coefficients. In the above equation, we ignore the term $\mathrm{d}n_\mathrm{e}/\mathrm{d}t$ since we assume the electron density changes much more slowly than the electron temperature and the time derivative of electron density is much smaller than the derivative of electron temperature.

author's e-mail: murakami.izumi@nifs.ac.jp

*) This article is based on the presentation at the 20th International Toki Conference (ITC20).

We also ignore the effect of recycling of gas and heat flux from the core plasma for simplicity.

Parameters of the calculations are impurity gas puff rate, and initial electron temperature and density. We assume the impurity gas is injected as neutral atoms with a constant rate and the puff is stopped at $t = 0.01$ s. We take the gas puff rate $dn(0)/dt = R_{puff}$ as $10^{12} \sim 10^{13}$ cm^{-3}s^{-1} and the final impurity fraction is $10^{-3} \sim 10^{-2}$. The initial electron density is assumed to be 10^{13} cm^{-3} and hydrogen is initially fully ionized. The initial electron temperature $T_e(0)$ is taken as 10-300 eV. If the neon atom and ions are in ionization equilibrium, the radiation power coefficient has maximum at around electron temperature 30 eV due to Ne^{6+} and Ne^{7+} ions and line radiation is dominant.

3. Time Evolution

We performed numerical calculations for several cases with parameters (R_{puff}, $T_e(0)$) described in Table 1.

Figure 1 shows time evolution of number densities and fractional abundance of Ne atom and ions for the case of $R_{puff} = 10^{13}$ cm^{-3}s^{-1} and $T_e(0) = 10$ eV (case a in Table 1). Until $t = 0.01$ s, Ne gas is injected and total Ne density increases. Ionization of Ne atom and ions proceeds to higher ionization stages until $t \sim 3 \times 10^{-3}$ s; it reverses after that due to decrease of electron temperature as shown in Fig. 2 with solid line (labeled with "a"). After the gas puff ends, the ion fractions quickly relax to ionization equilibrium and neutral fraction decreases quickly. Then due to decreasing electron temperature, Ne ions recombine and the neutral fraction increases. Neutral hydrogen density also increases due to the decreasing electron temperature. As seen in Fig. 1 neutral hydrogen density becomes comparable with electron density and we could expect that plasma detachment would be achieved in this case after $t \sim 0.62$ s. At that time, the electron temperature reaches 0.2 eV and electron density decreases to 5.6×10^{12} cm^{-3}.

Table 1 Parameter sets for the calculations and obtained integrated radiation power loss until $t = 1.5$ s.

case	R_{puff} (cm^{-3}s^{-1})	$T_e(0)$ (eV)	total loss (Jcm^{-3})
a	10^{13}	10	2.31×10^{-5} *
b	10^{13}	30	7.19×10^{-5} *
c	10^{13}	100	2.49×10^{-4}*
d	10^{13}	300	7.76×10^{-4}*
e	10^{12}	10	1.76×10^{-5}
f	10^{12}	30	6.58×10^{-5}
g	10^{12}	100	2.35×10^{-4}
h	10^{12}	300	2.20×10^{-4}

* integrated until the time shown in Fig. 2.

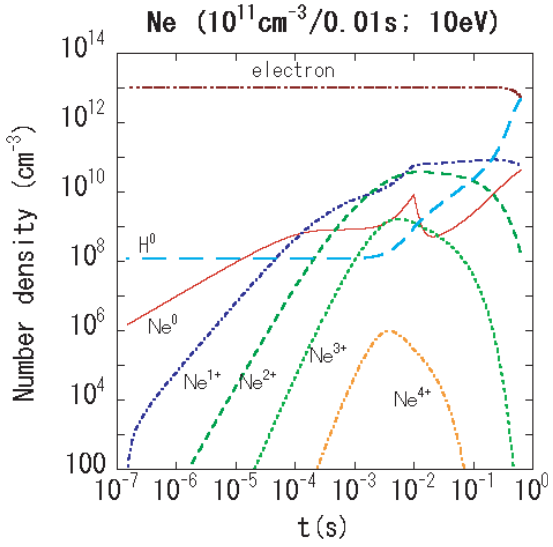

Fig. 1 Time evolution of number densities of Ne atom and ions, H neutral atom, and electron for the case a with $R_{puff} = 10^{13}$ cm^{-3}s^{-1} and $T_e(0) = 10$ eV.

Figure 2 shows time evolution of electron temperature for several cases. The cases with $R_{puff} = 10^{13}$ cm^{-3}s^{-1} are labeled a-d, and the cases with $R_{puff} = 10^{12}$ cm^{-3}s^{-1} are labeled e-h in Fig. 2, as in Table 1. As seen in Fig. 2, the cases with $R_{puff} = 10^{13}$ cm^{-3}s^{-1} (a-d) electron temperature falls below 1 eV and we could expect to have plasma detachment. Especially in the case of $T_e(0) = 100$ eV (case c), electron temperature decreases very quickly. On the other hand, in the cases with $R_{puff} = 10^{12}$ cm^{-3}s^{-1} (e-h) electron temperature does not drop below 1 eV even at $t = 1.5$ s. Especially in case h with $T_e(0) = 300$ eV, the radiation power loss is not sufficient, and the electron temperature does not decrease and is still higher than 100 eV at $t = 1.5$ s.

Figure 3 shows time evolution of total radiation power per unit volume due to all Ne atom and ions, i.e. $\sum_i L_{tot}(i) n(i) n_e$, summed for all ionic stages. The total radiation power increases until $t = 0.01$ s, except for cases a and b, in which power reaches the maximum at $t = (3 \sim 4) \times 10^{-3}$ s and decreases due to the change of ion fractions caused by electron temperature decrease. In case

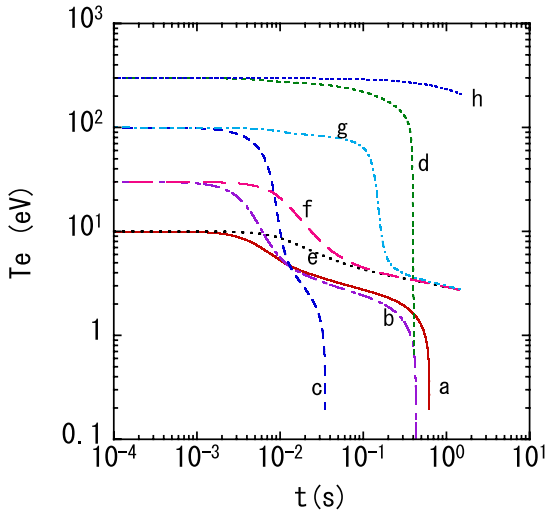

Fig. 2 Time evolution of electron temperature for the cases a-h described in Table 1.

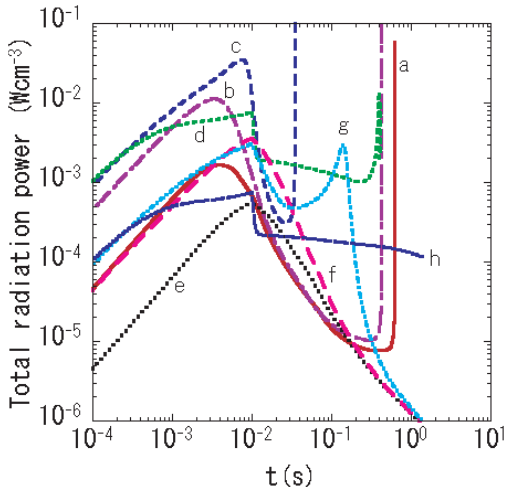

Fig. 3 Time evolution of total radiation power for the cases a-h described in Table 1.

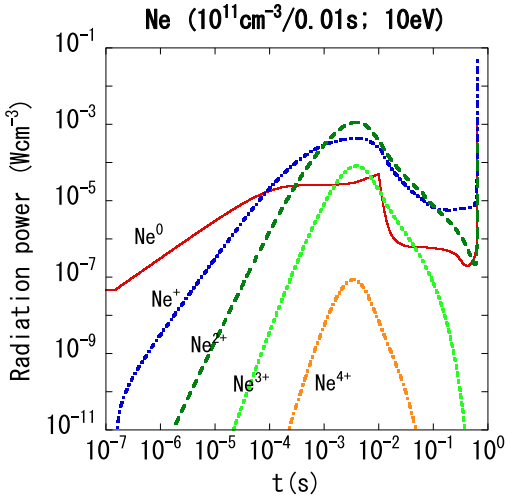

Fig. 4 Time evolution of radiation power due to each ion for the same case as in Fig. 1 (case a).

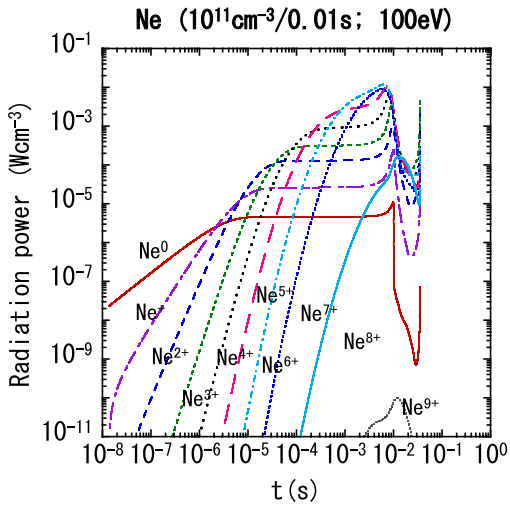

Fig. 5 Time evolution of radiation power due to each ion for the case c with $R_{\rm puff} = 10^{13}$ cm^{-3} and $T_{\rm e}(0) = 100$ eV (case c).

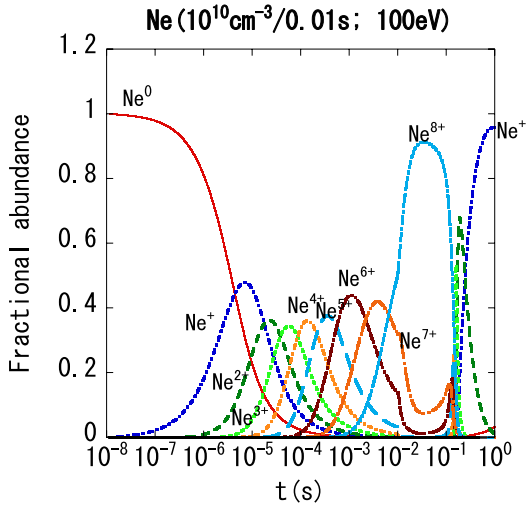

Fig. 6 Time evolution of fractional abundance for the case with ($R_{\rm puff} = 10^{12}$ cm^{-3}s^{-1} and $T_{\rm e}(0) = 100$ eV (case g).

a, Ne^{2+} ion contributes the maximum radiation power at $t \sim 3 \times 10^{-3}$ s as seen in Fig. 4. Figure 4 shows time evolution of radiation power of each ion, $L_{\rm tot}(i)n(i)n_{\rm e}$. Case c also has a power maximum before $t = 0.01$ s and the maximum power is the highest among the cases examined here. The time evolution of radiation power of each ion of this case is shown in Fig. 5 and $Ne^{5+} \sim Ne^{7+}$ contribute to the maximum radiation power. This leads to a rapid decrease of the electron temperature as seen in Fig. 2.

The radiation powers of the cases e-h become very low at $t = 1$ s as seen in Fig. 3 and the electron temperature decrease is very slow as seen in Fig. 2. It is difficult to expect to achieve detachment in these cases. The evolution of the ion fractional abundance for case e, which has the same initial electron temperature as case a, is similar to case a. However, because the gas puff rate and total neon density are one order smaller and the total radiation power of this case is one order smaller than for case a as seen in Fig. 4, and the decrease of electron temperature is slower than for case a. For case g, the total radiation power has two peaks, at $t = 0.01$ s and $t = 0.13$ s. After the termination of gas puffing at $t = 0.01$ s, Ne^{8+} ion is most abundant as seen in Fig. 6 because of the high electron temperature, but the radiation power is small as seen in Fig. 7. Thus the total radiation power decreases after $t = 0.01$ s. According to the decrease of electron temperature, ion fraction distribution changes and $Ne^{3+} \sim Ne^{7+}$ ions contribute to the total radiation power to make the second peak, which results in a rapid decrease of the electron temperature to reach 2.76 eV at $t = 1.5$ s.

4. Discussion and Conclusion

Examining the results described in Sec. 3, we found that the condition for plasma detachment, i.e. electron tem-

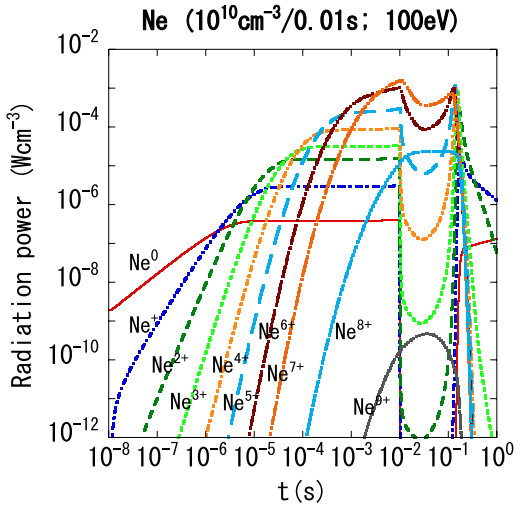

Fig. 7 Time evolution of radiation power of each ion for the same case as in Fig. 6 (case g).

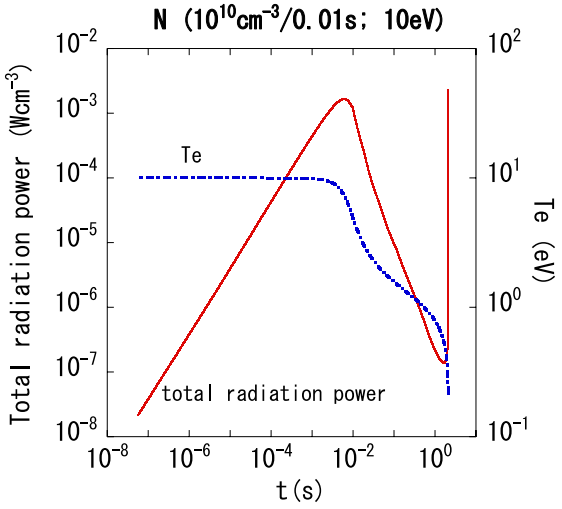

Fig. 8 Time evolution of total radiation power and electron temperature for nitrogen case with $R_{puff} = 10^{12}\,cm^{-3}$ and $T_e(0) = 10\,eV$.

perature falling below 1 eV in this work, depends on the gas puff rate and does not depend on initial electron temperature in the temperature range of 10-300 eV. In Table 1 we list the integrated radiation power until $t = 1.5$ s or the time when the calculation ends for the cases a-d. It is found that the integrated power with the same initial temperature is about the same even for different gas puff rates, except for the 300 eV cases. This also indicates that the condition that the electron temperature decreases to be less than 1 eV does not depend on the total energy density exhausted by radiation, but on the time history of ion densities and radiation power. For the cases a-d, the radiation power increases rapidly at the final stage of the calculations as seen in Fig. 3. This behavior might indicate that radiation collapse is induced and we need to consider the effect carefully in a more realistic model with special distribution of a plasma.

As a preliminary work, we calculated the case with nitrogen gas puff. Nitrogen molecular binding is not considered in the calculation. We found that the electron temperature becomes less than 1 eV at $t = 1$ s with the gas puff rate $10^{12}\,cm^{-3}s^{-1}$ for nitrogen case as shown in Fig. 8. This indicates that nitrogen cools the plasma more effectively with a smaller gas puff rate than neon. Of course we should include nitrogen molecules to calculate ion densities and this may change the time evolution of electron temperature.

In this work we ignore the effects of diffusion and recycling of impurities and heating due to high energy particles from core plasma moving along magnetic fields as well as the time derivative of electron density in the energy conservation equation, Eq. (2). These effects may change the time evolution of electron temperature and the condition for plasma detachment and we need to include these effects in future work.

Concluding this work, we performed calculations of time evolution of ion densities and electron temperature for several cases in order to examine the effect of radiation power loss due to impurity gas puff for a divertor plasma. We found the electron temperature becomes less than 1 eV for the cases with gas puff rate $10^{13}\,cm^{-3}s^{-1}$ during 0.01 s (in this case the final impurity fraction is 10^{-2}) but not for the cases with $10^{12}\,cm^{-3}s^{-1}$, independent of the initial electron temperature. If the electron temperature becomes less than 1 eV, hydrogen ions will recombine with electrons and we can expect to have plasma detachment.

Acknowledgement

This work is supported by the NIFS FFHR project. We appreciate Prof. R. M. More for reading the manuscript carefully.

[1] A. Sagara *et al.*, Fusion Eng. Des. **83**, 1690 (2008).
[2] D.E. Post, J. Nucl. Mater. **220-222**, 143 (1995).
[3] D.E. Post, N. Putvinskaya, F.W. Perkins and W. Nevins, J. Nucl. Mater. **220-222**, 1014 (1995).
[4] D.E. Post, J. Abdallah and R.E. Clark, N. Putvinskaya, Phys. Plasmas **2**, 2328 (1995).
[5] M.E. Rensink and T.D. Rognlien, LLNL Report, UCRL-ID-124702 (1996).
[6] M.E. Rensink, T.D. Rognlilen and D.D. Hua, LLNL Report, UCRL-ID-124702-1 (1997).
[7] Y. Suzuki *et al.*, Contrib. Plasma Phys. **48**, 169 (2008).
[8] G.S. Voronov, Atomic Data Nucl. Data Tables **65**, 1 (1997).
[9] P. Mazzotta *et al.*, Astron. Astrophys. Suppl. **133**, 403 (1998).
[10] D.A. Verner, http://www.pa.uky.edu/~verner/fortran.html (1999).
[11] H.P. Summers, The ADAS User Manual, version 2.6, http://www.adas.ac.uk (2004).